

# Continuous Wave Hydrogen Fluoride Overtone Lasing Saturation Effects on Fundamental Gain Suppression

P. T. Theodoropoulos,\* L. H. Sentman,<sup>†</sup> D. L. Carroll,<sup>‡</sup> R. E. Waldo,\* S. J. Gordon,\* and J. W. Otto\*  
*University of Illinois at Urbana-Champaign, Urbana, Illinois 61801*

A new technique that uses a multiline probe beam to measure the gain on several lines simultaneously was developed. This new technique was used to measure the gains of the fundamental lines  $P_1(4-9)$  and  $P_2(4-9)$  while lasing on the overtone, for three levels of medium saturation. For relatively high-medium saturation, obtained with 99.7/99.7% reflective mirrors, the gains of the low  $J$  lines  $P_1(4-6)$  and  $P_2(4-6)$  were suppressed 41–96%; the gains of the high  $J$  lines  $P_1(7-9)$  and  $P_2(7-9)$  were suppressed 3–44%. The  $1 \rightarrow 0$  lines were suppressed more than the  $2 \rightarrow 1$  lines. The maximum suppression occurred between 2 and 6 mm downstream from the nozzle exit plane, near the center of the 9-mm overtone beam. The suppression obtained with 99.8/99.86% reflective mirrors, which resulted in 55% larger intracavity flux, was essentially the same as that obtained with the 99.7/99.7% mirrors. For low-medium saturation, obtained with 98.0/99.7% reflective mirrors, there was essentially no suppression of the fundamental gains.

## I. Introduction

THE gains of the hydrogen fluoride (HF) fundamental  $2 \rightarrow 1$  and  $1 \rightarrow 0$  transitions are almost two orders of magnitude larger than the gains of the  $2 \rightarrow 0$  overtone transitions. To obtain lasing on the overtone, the fundamental must be suppressed.<sup>1</sup> The fundamental transitions are suppressed through the use of selective mirror coatings, i.e., the mirrors are less than 1% reflective at the fundamental wavelengths and greater than 99% reflective at the overtone wavelengths.<sup>1–4</sup> When the overtone laser is scaled to large gain lengths, even though the fundamental mirror reflectivities are less than 1%, the fundamental transitions may start to lase and/or amplified spontaneous emission (ASE) may reach levels that would substantially limit the performance of the device.<sup>5,11</sup> The occurrence of these phenomena will depend on the magnitude of the fundamental gains while lasing on the overtone, called the residual fundamental gain (RFG). Thus, the magnitude of the RFG may present a scaling limitation of the overtone laser.

The fundamental gain suppression due to overtone lasing is determined by comparing the residual fundamental gain with the zero power gain (ZPG). This study of residual fundamental gain was performed on the University of Illinois (UI) small-scale, supersonic continuous wave (cw) HF chemical laser<sup>6</sup> (SSL). The UI SSL zero power gains were measured<sup>7</sup> for lines  $P_1(4-8)$  and  $P_2(4-8)$ . These ZPG measurements were performed with a single-line probe beam. Since the SSL RFG measurements were to be performed for several lines and at several levels of medium saturation, a faster and more efficient method for measuring zero power and residual fundamental gain was needed. A new technique that uses a multiline probe beam to measure the gains of several lines simultaneously was developed. A by-product of the verification of the new multiline technique was the measurement of the ZPGs of lines  $P_1(9)$  and  $P_2(9)$ . A detailed discussion of the multiline gain measurement technique is presented in Sec. 11.

The SSL residual fundamental gains were measured for the peak gain lines  $P_1(4-9)$  and  $P_2(4-9)$  with a pair of 99.7/99.7% reflective overtone mirrors, Sec. III. These were the mirrors that gave the best overtone efficiency.\* The gains of the low  $J$  lines  $P_1(4-6)$  and

$P_2(4-6)$ , whose upper or lower levels were not directly involved in overtone lasing, were suppressed more than the gains of the high  $J$  lines  $P_1(7-9)$  and  $P_2(7-9)$ , whose upper or lower levels were directly involved in overtone lasing.

To determine the effect of medium saturation, the residual fundamental gains were measured for two additional levels of medium saturation. Experiments were performed at low-medium saturation with 98.0/99.7% reflective overtone mirrors and at high-medium saturation with 99.8/99.86% reflective overtone mirrors, Sec. IV.

## II. Multiline Zero Power Gain Measurement Technique

Zero power gain measurements in cw HF chemical lasers are usually performed using a single-line probe beam. The wavelength of the probe beam is the same as that of the line whose gain is to be measured. Once the gain measurements for a given transition have been completed, as a function of location in the flowfield, the entire procedure (including alignment) must be repeated to measure the gain of another transition. If the gains of several lines are to be measured, this method can be time consuming and, in the case of large-scale devices, costly in terms of gases. A faster and more efficient method for measuring zero power gain would be to use a multiline probe beam to measure the gains of several lines simultaneously.

When the input intensity of each line in a multiline probe beam is low enough that all lines are in the zero power gain region, it should be possible to use a multiline probe beam to perform the zero power amplification ratio (ZP-AR) measurements. The scanning monochromator would record the spectra with  $H_2$  on and with  $H_2$  off. The ratio of the spectral peaks for each line would give the amplification ratio of each line. Since the input beam would contain several lines, this would speed up the gain measurements. To determine the feasibility of using a multiline probe beam to measure zero power gain, supersonic laser ZP-AR measurements were performed for lines  $P_1(6-9)$  and  $P_2(7-9)$  using a multiline probe beam and were compared to the single-line measurements.

A schematic of the layout used for the multiline ZP-AR and the residual fundamental gain amplification ratio (RF-AR) measurements is presented in Fig. 1. The Helios CLI probe laser used a stable resonator composed of a 2-m concave enhanced total reflector (ETR) and a 44.5% reflective 2-m concave outcoupler. Since a parallel probe beam is necessary to perform the zero power gain measurement: a telescope was used to produce a parallel probe beam 18 mm in diameter. The multiline probe beam was aligned 5 mm downstream from the nozzle exit plane at the centerline of the flow channel.

As the input intensity decreases, the gain increases until at some point, it becomes equal to the zero power (small signal) gain.

Received Jan. 20, 1994; revision received July 19, 1995; accepted for publication July 26, 1995. Copyright © 1995 by the American Institute of Aeronautics and Astronautics, Inc. All rights reserved.

\*Research Assistant, Aeronautical and Astronautical Engineering Department.

<sup>†</sup>Professor, Aeronautical and Astronautical Engineering Department. Associate Fellow AIAA.

<sup>‡</sup>Postdoctoral Research Associate, Aeronautical and Astronautical Engineering Department. Member AIAA.

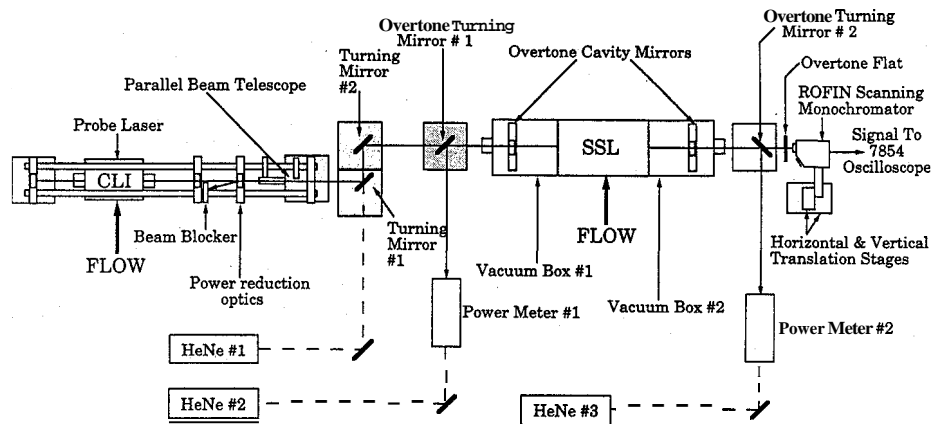
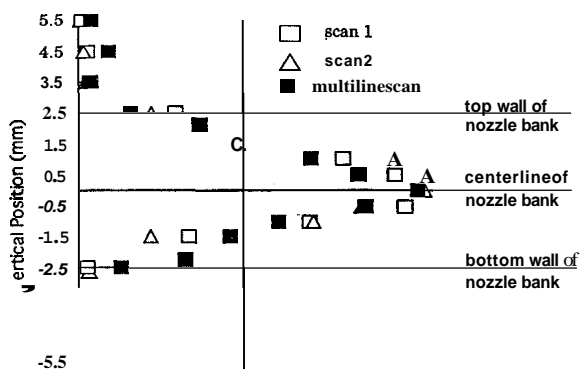


Fig. 1 Schematic of the experimental layout for the zero power and residual fundamental gain studies.



lines.<sup>7,9</sup>

with the fundamental  $1 \rightarrow 0$  transitions, lasing on the overtone should result in a decrease of the fundamental gains. To determine the extent to which this occurs, the supersonic laser RF-ARs were measured for the peak zero power gain lines  $P_1(4-9)$  and  $P_2(4-9)$  while the laser was operating on the overtone lines  $P_{20}(8-11)$ . These measurements were performed with 99.7% reflective overtone mirror sets, which gave the largest overtone power and efficiency.'

#### A. Experimental Procedure

The layout of the residual fundamental gain experiment is shown in Fig. 1. A set of conditions at which the probe laser would provide a beam with all  $P_1(4-9)$  and  $P_2(4-9)$  lines lasing simultaneously could not be found. Thus, the RF-AR measurements were performed in two sets, first for the high  $J$  lines,  $P_1(7-9)$  and  $P_2(7-9)$ , and then for the low  $J$  lines,  $P_1(4-6)$  and  $P_2(4-6)$ .

The infrared (IR) probe beam was aligned through the SSL flow channel 10 mm downstream from the nozzle exit plane. This was accomplished by the following procedure. Two aluminum plates inscribed with vertical and horizontal scales in increments of 1 mm were designed to fit around the vacuum box (VB) apertures on both sides of the laser to allow accurate measurement of the beam location relative to the SSL nozzle exit plane and flow channel. The horizontal and vertical adjustment knobs on turning mirrors 1 and 2 were used to align the beam at the center of the flow channel, 10 mm downstream from the nozzle exit plane.

Once the probe beam was aligned 10 mm downstream from the nozzle exit plane, the parallel beam telescope, with two-axis translation capability at both of its ends, was mounted on the optical bars on the output side of the probe laser, as shown in Fig. 1, without any lenses in place. The telescope was aligned so that the probe beam passed along the centerline of the telescope body. This ensured that the beam passed through the center of the lenses when they were inserted in the telescope, thus minimizing any optical aberration effects.

The next step was to insert the 100-mm-radius plano-convex calcium fluoride ( $\text{CaF}_2$ ) lens at the output end of the telescope. This lens focused the beam down to a small point. Small adjustments of the translation stages at the output end of the telescope were used to correct the alignment without affecting the centering of the beam in the telescope.

With the plano-convex lens in place, the 20 mm radius of curvature plano-concave  $\text{CaF}_2$  lens at the input end of the telescope was inserted. This lens diverged the input beam while the plano-convex lens focused the beam, which produced a slightly converging beam to correct for the fact that the concave overtone cavity mirror in VB 1 acts as a diverging optical element. The horizontal and vertical knobs of turning mirrors 1 and 2 were then adjusted until the probe beam was centered in the flow channel, 10 mm downstream from the nozzle exit plane.

To provide a visible reference for the location of the IR probe beam, helium-neon laser (HeNe) 2 was aligned with the center of

the IR probe beam. When overtone turning mirror 1 was inserted, the only effect that this mirror had on the IR probe beam was to shift the beam 2 mm upstream. This was corrected by translating turning mirror 2 downstream 2 mm. Overtone turning mirror 1 was aligned to provide a HeNe beam that was centered in the flow channel 10 mm downstream from the nozzle exit plane and that was collinear and centered with the IR probe beam.

The 4-m concave (CC) overtone mirror was placed in VB 1, centered with respect to the IR and HeNe beams and aligned from its back surface with the HeNe beam. A power reduction optic (a 73% R, 2-m CC outcoupler) was used to reduce the peak intensity below the threshold input intensity required for zero power gain measurements. The reflected portion of the probe beam was deposited on a ceramic beam blocker as shown. The alignment of the probe beam through the SSL was again checked to ensure that the beam was centered in the flow channel, 10 mm downstream from the nozzle exit plane. The probe beam was aligned by centering the IR beam at the input side of vacuum box 1 to the HeNe beam that was already aligned with the flow channel. This was accomplished by viewing both beams on a thermal image plate at the input side of vacuum box 1. A 2-mm-thin Plexiglas plate was taped at the output side of VB 2, against the aluminum plate with the 1 mm horizontal and vertical scales that was designed to provide a reference for the position of the beam with respect to the nozzle exit plane and flow channel. The Plexiglas plate was kept taped on the vacuum box until a burn was formed on it by the low intensity probe beam. The alignment of the probe beam was then checked by comparing this burn to the marks on the aluminum plate. Any necessary adjustments of turning mirrors 1 and 2 were performed to correct the alignment. This procedure was repeated until the probe beam was aligned through the SSL.

With all of the optical elements in place, the spacing between the lenses of the telescope was adjusted to provide a parallel beam after the first overtone cavity mirror. To establish the parallelism of the probe beam, horizontal and vertical intensity profiles were measured for lines  $P_1(4-9)$  and  $P_2(4-9)$  at the right window, denoted near field (NF), and 18 cm away from the right window, denoted far field (FF). Comparison of these profiles showed that a parallel probe beam was passed through the cavity parallel to the optical axis for all lines.<sup>10</sup> These intensity profile measurements were performed before the second overtone cavity mirror and the optical elements on the right-hand side of the SSL were installed.

To sample the entire gain region, turning mirror 2, overtone turning mirror 1, and the cavity mirror in VB 1 were translated 5.0 mm upstream to place the center of the IR probe beam 5.0 mm downstream from the nozzle exit plane. To determine if earlier ZP-AR data<sup>7</sup> could be reproduced with the current setup, zero power amplification ratio measurements were performed at 2.0 and 6.0 mm downstream from the nozzle exit plane. There was good agreement between the present and previous zero power amplification ratio data.<sup>10</sup> This proved that the SSL performance was the same as during the earlier ZP-AR measurements? which means that the RF-AR results can be compared to the existing ZP-AR data to determine the suppression due to overtone lasing.

The second overtone turning mirror (on the right-hand side, Fig. 1) was installed and horizontal and vertical near- and far-field intensity profiles were taken to determine the effect of the turning mirror on the parallelism and alignment of the probe beam. These data showed that the only effect of this turning mirror was to shift the probe beam 2 mm downstream in the horizontal direction. This horizontal shift of the probe beam did not affect the experiment because the monochromator's field of view with respect to the flowfield was determined with the turning mirror in place.

The first overtone cavity mirror was removed from VB 1 and the HeNe 3 laser was installed and aligned through the SSL 5.0 mm downstream from the nozzle exit plane so that it overlapped with HeNe 2 laser, Fig. 1. The first overtone cavity mirror was placed in VB 1 and aligned from both its front and back surfaces using the two HeNe lasers. The alignment of the probe beam was checked and corrected. The second overtone cavity mirror was placed in VB 2 and aligned using HeNe 3. Horizontal and vertical far-field intensity profiles were obtained before and after the installation of the second overtone cavity mirror to determine the effect that this mirror has on the probe beam. Comparison of the  $P_1(8)$  horizontal and vertical

far-field intensity profiles showed that the second overtone mirror expands the probe beam by 4 mm in the horizontal direction and 2.5 mm in the vertical direction."

Since the right overtone cavity mirror in VB 2 is concave, it caused the probe beam to diverge as described earlier. To compensate for this, the micrometer readings of the horizontal and vertical translation stages (which position the monochromator) corresponding to specified horizontal and vertical locations in the optical cavity were determined and recorded." This technique allowed the monochromator to be positioned to view the desired  $x, y$  locations in the optical cavity in the plane perpendicular to the optical axis while the SSL was lasing on the overtone.

At the beginning of the RF-AR measurements, it was found that the overtone power transmitted through overtone turning mirror 2 was sufficient to excite the monochromator detector used to measure the RF-ARs. To prevent this from happening, a flat overtone mirror with 99.7% overtone reflectivity and 92.8% fundamental transmissivity was placed in front of the monochromator, Fig. 1.

The SSL was run with the probe laser off with the 4-m CC overtone cavity mirrors to determine if the overtone performance could be reproduced. The output power was 10.3 W with lines  $P_{20}(7-10)$  lasing with the peak at  $P_{20}(8, 9)$ . Since both the SSL overtone power and spectra were reproduced, it was possible to proceed with preliminary RF-AR measurements.

With the SSL off, the probe laser was turned on and the probe beam power and spectra were examined to ensure that they satisfied the conditions necessary for RF-AR measurement. The probe laser spectra contained lines  $P_1(7-9)$  and  $P_2(7-9)$ . After overtone turning mirror 1, the probe beam was 15 mm in diameter with a power of 1.5 W. This provided a multiline probe beam with single-line intensities that were below the threshold input intensity of 0.59 W/cm<sup>2</sup> required for gain measurements.

The SSL was run with the probe laser on to determine the effect that the probe laser has on SSL performance. The overtone power was 7.5 W with lines  $P_{20}(8-11)$  lasing with the peak at  $P_{20}(8, 9)$ . All values presented for output power include corrections for window and turning mirror losses. The SSL pressure upstream and downstream of the nozzle bank was 18.2 torr and 5.44 torr, respectively. The 0.34 torr increase in SSL cavity pressure that resulted from turning on the probe laser caused a significant decrease in SSL output power and shifted the spectra one  $J$  higher. The measured overtone beam size was 4.0 mm high and 9.0 mm long on both sides of the SSL. The increase in the cavity pressure of the SSL when the probe laser was operating was due to the fact that the vacuum system was not able to pump the increased mass flow due to the probe laser and keep the SSL cavity pressure at 5.1 torr. Since this pressure increase occurred when the zero power gains were measured, the conditions in the laser cavity were identical for both the zero power and the residual fundamental gain measurements. Thus, the zero power and residual fundamental gains may be compared to determine the amount of suppression due to overtone lasing. Since the vacuum system could not maintain 5.1 torr in the SSL cavity when the probe laser was operating, it was not possible to determine the effect of the increased cavity pressure on the suppression of the fundamental gains.

## B. Residual Fundamental Amplification Ratio Measurements with Two 99.7% Reflective Overtone Mirrors

Two sets of RF-AR data were taken at 0.5, 2, 4, 6, 8, and 10 mm downstream from the nozzle exit plane as a function of vertical position in the flow channel with a pair of 99.7% reflective overtone mirrors ( $\alpha_{\text{sat}} = 0.00010015$ ,  $L_g = 30$  cm).

To determine the effect of overtone lasing on the fundamental gains, the RF-AR data were compared to the corresponding ZP-AR data. At each  $(x, y)$  point, the ZP-AR scans were averaged. The RF-AR scans were compared with the averaged ZP-AR vertical profiles at each  $x$ . (The RF-AR data were obtained with two 4-m concave 99.7% reflective mirrors.) Typical vertical scans for lines  $P_1(5)$  and  $P_2(8)$  are shown in Figs. 3 and 4. It is clear from these figures that the RF-AR data are quite reproducible and are generally lower than the ZP-AR data. Since it was not possible to obtain RF-AR data at the nozzle exit plane ( $x = 0.0$  mm) due to the low amplitude of the signal, the RF-AR data were obtained 0.5 mm downstream

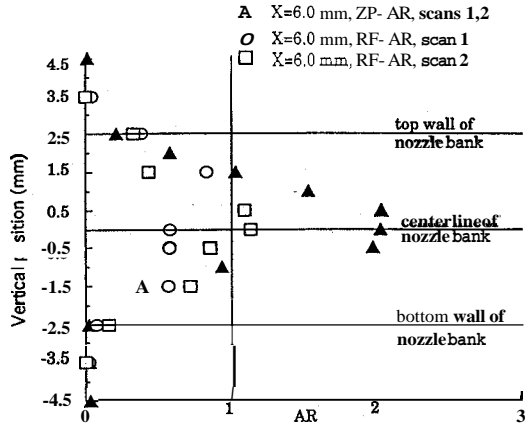


Fig. 3 Comparison of  $P_1(5)$  ZP-AR and RF-AR vertical scans at 6.0 mm downstream from the nozzle exit plane.

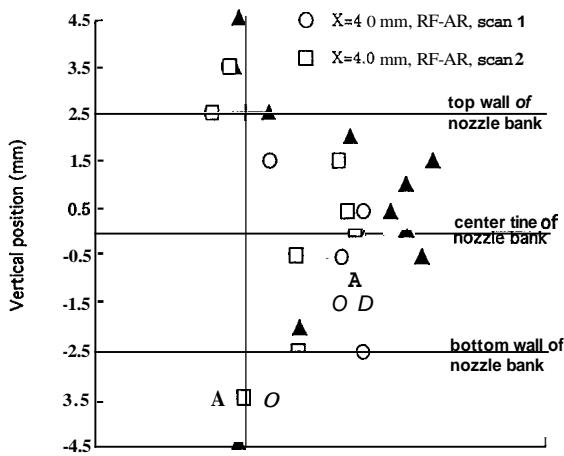


Fig. 4 Comparison of  $P_2(8)$  ZP-AR and RF-AR vertical scans at 4.0 mm downstream from the nozzle exit plane.

from the nozzle exit plane. As a result, the RF-AR data 0.5 mm downstream from the nozzle exit plane are higher than the ZP-AR data obtained at the nozzle exit plane. Examination of the ZP-AR and RF-AR data shows that the ZP-AR profiles have been suppressed, resulting in smoother gain profiles.

To quantify the fundamental gain suppression by overtone lasing and to present the data in a form suitable for comparison with computer model calculations, the RF-AR data were averaged in the vertical direction at each value of  $x$  and compared to the vertically averaged ZP-AR data. (The RF-AR data were obtained with two 4-m concave 99.7% reflective mirrors.) The averaged data are compared in Figs. 5 and 6. These figures show that the  $P_1(7-9)$  lines are generally suppressed more than the  $P_2(7-9)$  lines and that the low  $J$  lines,  $P_1(4-6)$  and  $P_2(4-6)$ , are suppressed more than the high  $J$  lines,  $P_1(7-9)$  and  $P_2(7-9)$ . Even though the low  $J$  lines are suppressed more than the high  $J$  lines, the peaks of the high  $J$  lines are suppressed as illustrated in Fig. 4.

The ratio of the residual fundamental gain to the zero power gain is calculated as follows. Since

$$AR_{ZP} = \exp(\alpha_{ZP} L_e) \quad (1)$$

where  $\alpha_{ZP}$  is the fundamental small signal gain coefficient at zero power and  $L_e$  is the thickness of the mixed flow in the direction of the optical axis at the point at which the amplification ratio is measured, and

$$AR_{RF} = \exp(\alpha_{RF} L_e) \quad (2)$$

Table 1 Ratio of residual fundamental gain to zero power fundamental gain based on the vertically averaged amplification ratios, 99.7/99.7 mirrors;  $RFG/ZPG = \ln(AR_{RF})/\ln(AR_{ZP})$

Line	Position downstream from the nozzle exit plane, mm <sup>a</sup>					
	0.0/0.5	2.0	4.0	6.0	8.0	10.0
$P_1(4)$	0.058	-0.195	-0.498	-0.828	-1.328	-1.995
	-0.571	0.018	0.152	0.113	—	—
$P_1(5)$	5.734	0.430	0.202	0.162	-0.457	-1.121
	—	—	—	0.402	—	-0.320
$P_1(6)$	2.288	0.834	0.466	0.427	0.389	-0.345
	—	—	—	—	—	0.160
$P_1(7)$	0.950	0.686	0.570	0.640	0.629	0.660
$P_1(8)$	1.932	0.658	0.682	0.616	0.806	0.794
$P_1(9)$	0.451	0.671	0.558	0.974	0.990	0.923
$P_2(4)$	0.975	0.037	-0.304	-0.616	-1.187	-1.737
	—	—	0.199	-0.347	—	—
$P_2(5)$	1.228	0.386	0.251	0.513	-0.596	-1.149
	—	—	—	—	—	—
$P_2(6)$	1.887	0.523	0.591	0.704	-0.207	-0.734
	—	—	—	—	-0.226	—
$P_2(7)$	0.827	0.611	0.825	1.159	1.923	0.107
	—	—	—	—	—	—
$P_2(8)$	1.368	0.998	0.723	0.927	1.518	0.053
	—	—	—	—	—	-0.213
$P_2(9)$	0.906	1.139	0.974	1.023	1.131	2.024

<sup>a</sup>Dashes denote that the data do not exist at these positions.

where  $\alpha_{RF}$  is the fundamental small signal gain coefficient while lasing on the overtone, the ratio of the gains is

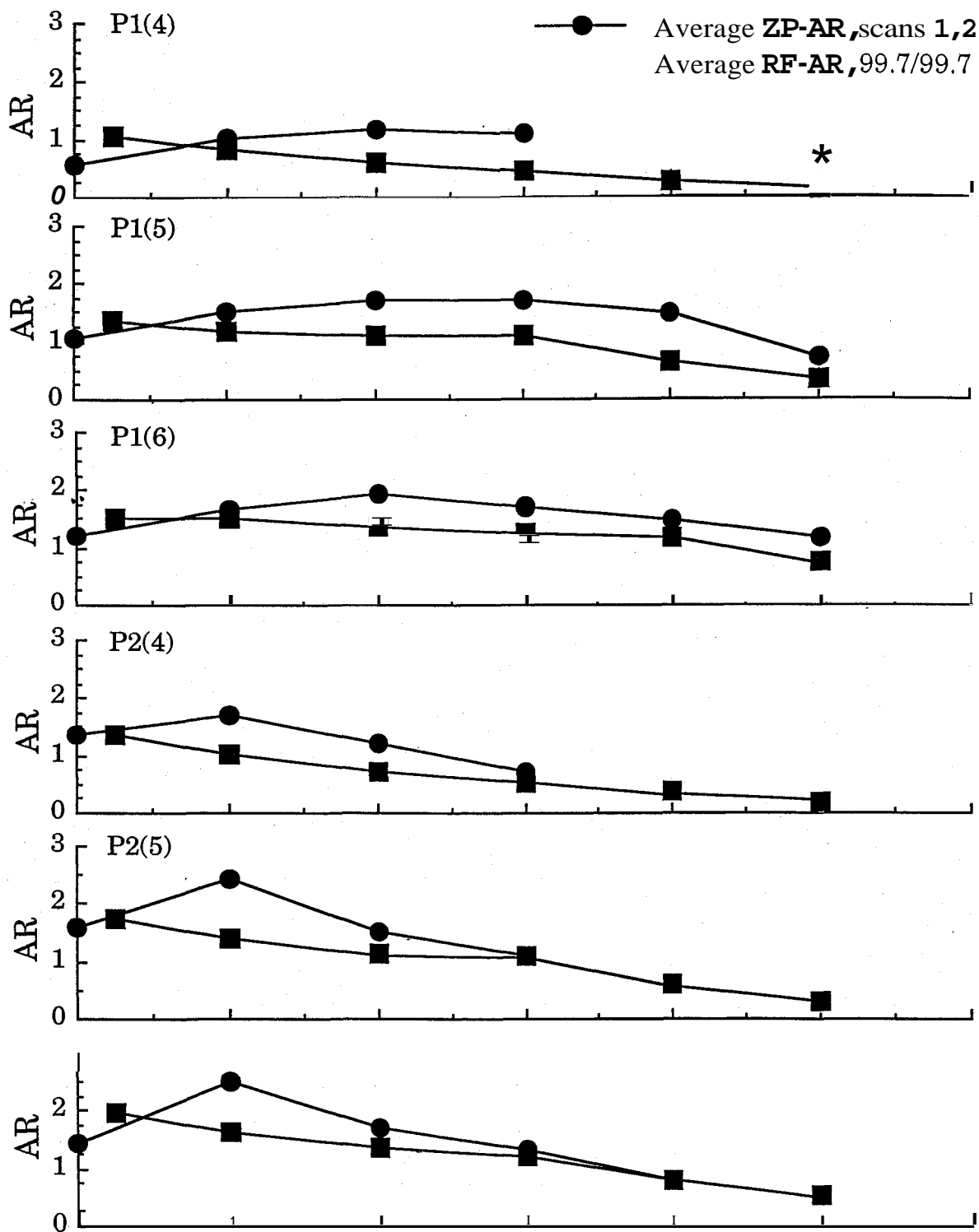
$$\frac{\alpha_{RF}}{\alpha_{ZP}} = \frac{\ln AR_{RF}}{\ln AR_{ZP}} \quad (3)$$

This ratio is tabulated for the averaged  $AR_{RF}$  and  $AR_{ZP}$  data for all lines in Table 1 as a function of position downstream from the nozzle exit plane. The ratio of  $\ln(RF-AR)/\ln(ZP-AR)$  was left as a fraction in some cases because either RF-AR or ZP-AR (or both) had values below 1.0, which results in negative  $\ln$ . This indicates absorption. The data were obtained with a pair of 99.7% reflective mirrors. From this table it is seen that the peak suppression ( $1 - \alpha_{RF}/\alpha_{ZP}$ ) of the low  $J$  fundamental gains varies between 41 and 96% and the peak suppression of the high  $J$  fundamental gains varies between 3 and 44%. For both low and high  $J$  lines, the maximum suppression occurred between 2 and 6 mm downstream from the nozzle exit plane. Since the measured overtone beam diameter was about 9.0 mm with its upstream edge at the nozzle exit plane, the maximum suppression of the fundamental gain occurred near the center of the overtone beam.

It should be noted that the low  $J$  46 lines are suppressed more than the high  $J$  7-9 lines. The laser was operating on the  $P_{20}(8-11)$  lines while these measurements were made. The upper and lower levels for these transitions are also the upper or lower levels for the  $P_2(8, 9)$  and  $P_1(8, 9)$  transitions, respectively, Fig. 7. The gains of these lines were suppressed by overtone lasing, as expected. The  $1 \rightarrow 0$  lines were suppressed more than the  $2 \rightarrow 1$  lines. There was minimal suppression of lines  $P_2(8, 9)$ . The surprising result was that the low  $J$  fundamental gains were suppressed more than the high  $J$  fundamental gains even though their upper or lower levels were not directly involved in overtone lasing. The reasons for this are discussed in Refs. 10 and 12.

#### IV. Residual Fundamental Gain Measurements as a Function of Medium Saturation

The scalability of the overtone laser to large gain lengths depends on the magnitude of the residual fundamental gain." To determine the variation of RFG with medium saturation, the RF-ARs were measured for a range of overtone reflectivities. The data generated by these experiments will provide the database needed to check computer model predictions of the residual fundamental gain profiles and fundamental gain suppression (Aa). The first set of RF-AR measurements was performed at a relatively high level of medium saturation with a pair of 99.7% overtone mirrors,  $\alpha_{sat} = 0.00010015$ . Residual fundamental amplification ratio measurements with



overtone resonators that provided a lower and a higher degree of medium saturation were performed. The results of these experiments are summarized in the following sections.

**A. Residual Fundamental Amplification Ratios with 99.7/98.0% Reflective Overtone Mirrors**

The residual fundamental amplification ratio measurements with an overtone resonator of low reflectivity were performed first. Computer simulation of RFG vs  $\sqrt{(R_1 \times R_2)}$  suggested that an overtone resonator with mirror reflectivities of 99.7 and 98.0%,

$\alpha_{sat} = 0.000386787$ , would provide minimal suppression of the fundamental gains.<sup>10,12</sup>

To establish that the SSL performance had not changed, ZP-AR measurements at 4.0 and 6.0 mm downstream from the nozzle exit plane for lines P<sub>1</sub>(7-9) and P<sub>2</sub>(7-9) were made. A comparison of these data with previously obtained single-line ZP-AR data showed that the SSL performance had not changed. Thus, the new RF-AR data can be compared with the existing ZP-AR data.

With the probe laser off and the 99.7/98.0% 4-m concave mirrors in vacuum boxes 1 and 2, respectively, the maximum overtone output

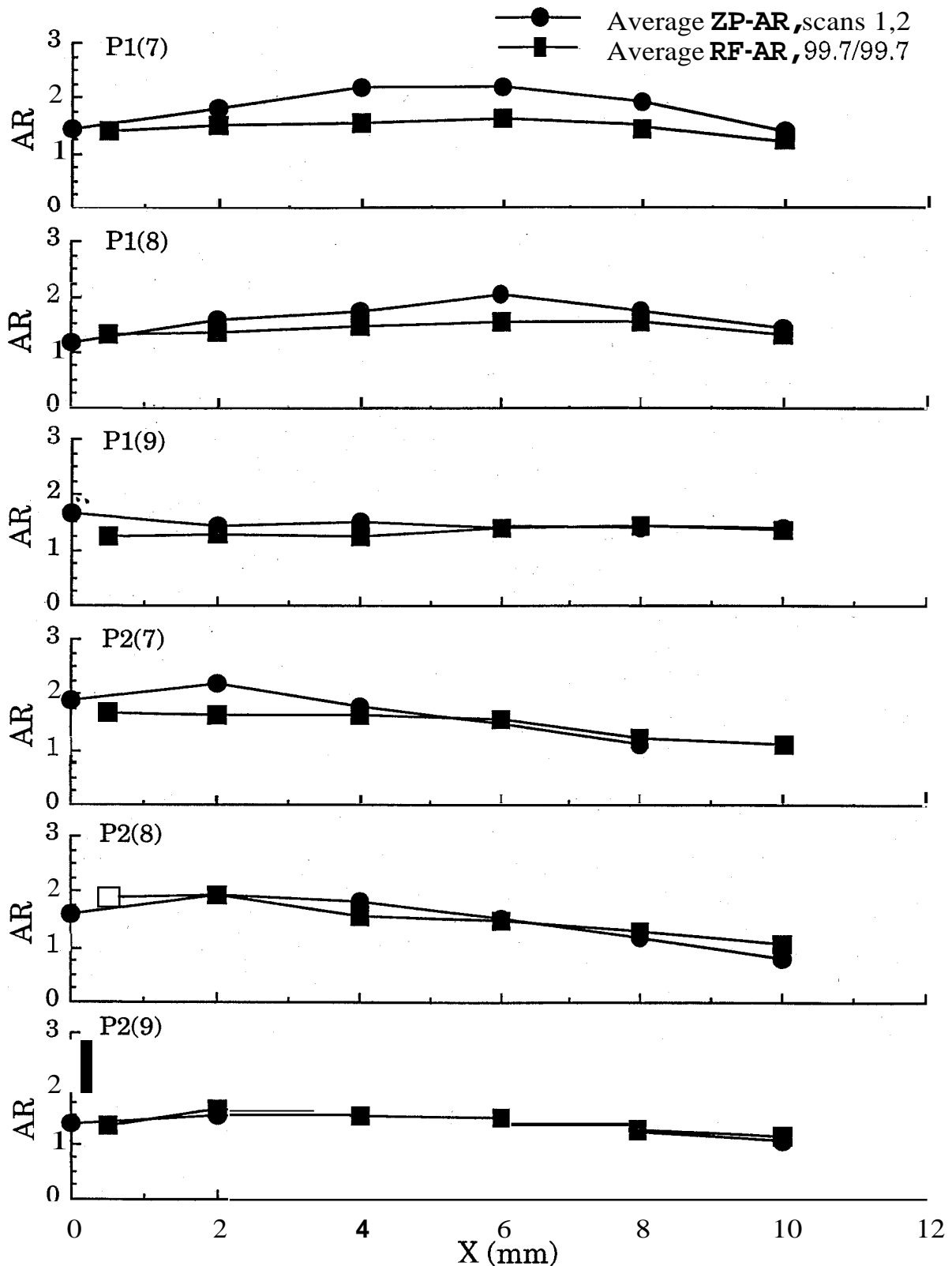


Fig. 6 Comparison of averaged ZP-AR and RF-AR data as a function of distance downstream from the nozzle exit plane,  $X$ .

power was 5.1 W with lines  $P_{20}(6-8)$  lasing. With the probe laser on, the maximum output power was 0.62 W. This relatively low-output power was due to the increased cavity pressure (5.4orr) that was a consequence of the mass flow limitations of the vacuum system. The low-resonator reflectivity and the increased cavity pressure cause the SSL to be close to the threshold of lasing, resulting in low-SSL overtone output power. The output power was monitored during the RF-AR experiments to ensure that the medium saturation did not change. The lines lasing in this case were  $P_{20}(7, 8)$ . Residual

fundamental amplification ratio data were obtained at this low level of medium saturation for axial positions of 0.5, 2, 4, 6, 8, 10, and 11 mm downstream from the nozzle exit plane as a function of vertical position in the flow channel.

To obtain a quantitative measure of the fundamental gain suppression by overtone lasing at these low-mirror reflectivities, the RF-AR data were averaged in the vertical direction at each axial position and compared to the averaged ZP-AR data.<sup>10</sup> In all cases the average ZP-AR and RF-AR data are close, indicating very little if

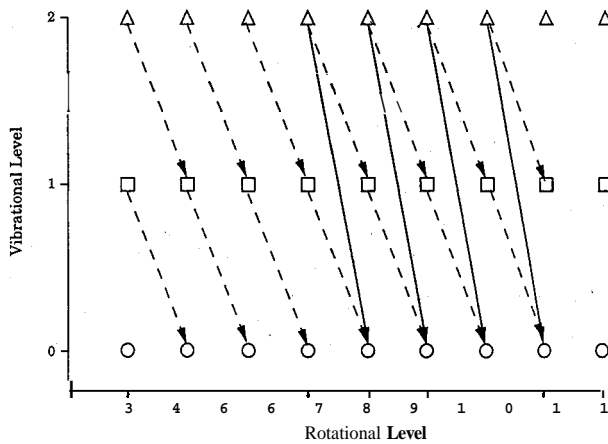


Fig. 7 Schematic of fundamental and overtone transitions for the HF chemical laser: solid arrows indicate the  $2 \rightarrow 0$  overtone transitions that were lasing during the RF-AR measurements, dashed arrows indicate the fundamental transitions whose RF-ARs were measured.

any suppression. There was weak suppression in the cases of  $P_1(7)$ ,  $P_2(5)$ , and  $P_2(6)$  between 2 and 6 mm downstream from the nozzle exit plane, whereas there was no clear indication of suppression in the case of the other lines. This supports the computer results of residual fundamental gain vs media saturation that showed that the fundamental gain suppression would be minimal in the SSL with overtone mirrors of  $R_1 = 0.98$  and  $R_2 = 0.997$  (Refs. 10 and 12).

#### B. Residual Fundamental Amplification Ratios with 99.8/99.86% Reflective Overtone Mirrors

Computer calculations<sup>10,12</sup> of residual fundamental gain and amplification ratio as a function of medium saturation indicated that above a reflectivity of 99.7%, the RF-AR does not change significantly with increased reflectivity even when the gain length is increased by a factor of two. To check the computer predictions and to determine the relation between medium saturation and residual fundamental gain, RF-AR data were obtained at an increased level of medium saturation with 99.8/99.86% mirrors ( $\alpha_{\text{sat}} = 0.000056716$ ). With the 99.8/99.86% mirrors the measured power spectral distribution contained lines  $P_{20}(7-12)$  (Refs. 8 and 10).

To quantify the comparison between the medium saturation obtained during the earlier RF-AR measurements and that obtained with these high-reflectivity mirrors, the intracavity flux and overtone efficiency<sup>8</sup> obtained in each case were calculated.<sup>10</sup> At a cavity pressure of 5.1 torr, the intracavity circulating power obtained was 12,396 W. Because of flow limitations of the laboratory vacuum system, the cavity pressure during the RFG measurements was 5.4 torr. At this pressure the SSL with the 99.8/99.86% mirrors produced 8.2 W and an intracavity circulating power of 8542 W. At the same cavity pressure, the intracavity circulating power for the 99.7/99.7% mirrors was 5716 W. This means that with the high reflectivity mirrors the intracavity flux increased about 50%. The ratio of  $\alpha_{\text{sat}}$  with the 99.8/99.86% mirrors to  $\alpha_{\text{sat}}$  with two 99.7% reflective mirrors is 0.566. The higher reflectivity mirrors result in an  $\alpha_{\text{sat}}$  that is 43.4% smaller than that of the 99.7/99.7% mirrors.

Earlier experiments had shown that the SSL gains change with run time. To correctly determine the fundamental gain suppression, the RF-AR data must be compared with the proper ZP-AR data. Two sets of low  $J$  ZP-AR vertical scans (scans 5 and 6) were obtained at 0.5, 2, 4, 6, 8, and 10 mm downstream from the nozzle exit plane. A comparison of these data with the existing ZP-AR data indicated good agreement for all lines except  $P_1(4)$  where the ARs were lower than those measured during earlier experiments. It has been experimentally determined that old anodes and cathodes have a pronounced effect on the  $P_1(4)$  line. This is probably due to the fact that  $P_1(4)$  is near threshold. The anodes and cathodes were changed and an additional set of ZP-AR data was obtained (scan 7) to correct for the low  $P_1(4)$  ARs in scans 5 and 6.

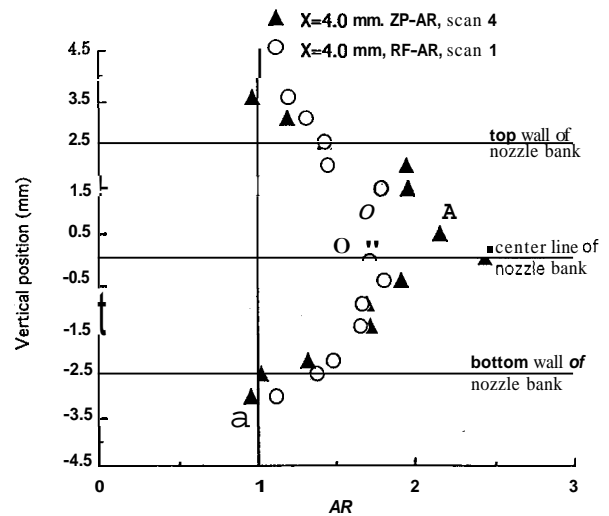


Fig. 8 Comparison of  $P_2(8)$  ZP-AR and RF-AR vertical scans at 4.0 mm downstream from the nozzle exit plane.

The SSL performance with the 99.8/99.86% mirrors was reproduced. Lasing was observed on lines  $P_{20}(7-12)$ , and the output power was 11.9 W. With the probe laser on, the SSL lased on lines  $P_{20}(8-12)$ , and the total output power was 8.5 W. With the probe beam properly aligned through the SSL, one set of ZP-AR and RF-AR vertical scans were obtained at 0.5, 2, 4, 6, 8, and 10 mm downstream from the nozzle exit plane. The RF-AR data obtained with a set of 4-m concave 99.8/99.86% mirrors were plotted with the averaged ZP-AR data to determine the suppression of the fundamental gains. Comparison of these ZP-AR and RF-AR profiles showed that the fundamental gains were suppressed due to lasing on the overtone, as illustrated in Fig. 8. The highest suppression occurred between 2 and 6 mm downstream from the nozzle exit plane. Comparison of these new data, with the data obtained with the two 99.7% mirrors, revealed that the suppression of the fundamental gains due to overtone lasing was about the same in both cases.

To quantify the fundamental gain suppression by overtone lasing and to present the data in a form suitable for comparison with computer model calculations, the RF-AR data were averaged in the vertical direction at each value of  $x$  and compared with the vertically averaged ZP-AR data. These data were plotted along with the corresponding average data obtained with the two 99.7% nominally reflective mirrors.<sup>10</sup> This comparison indicated that the suppression obtained with the 99.8/99.86% reflective mirrors and with the two 99.7% reflective mirrors is about the same for all lines. This indicates that the computer prediction that above a reflectivity of 99.7% the RF-AR does not change significantly with increased reflectivity<sup>10,12</sup> agrees with the experiment.

#### V. Concluding Remarks

The main objective of this work was to determine the extent to which lasing on the overtone suppresses the gain on the fundamental transitions  $P_1(4-9)$  and  $P_2(4-9)$  as a function of medium saturation on the overtone. This was accomplished by a comparison of the residual fundamental gain data obtained at three different levels of medium saturation with the corresponding zero power gain data.

A new technique that uses a multiline probe beam to measure the gain on several lines simultaneously was developed. The agreement between the single-line and multiline zero power amplification ratio data for lines  $P_1(6-8)$  and  $P_2(7, 8)$  verified this new technique. Since the multiline probe beam contained the lines  $P_1(9)$  and  $P_2(9)$ , ZP-AR data were obtained for two lines for which single-line data had not previously been obtained.

The first set of RF-AR data was obtained at a relatively high-medium saturation with two nominally 99.7% reflective mirrors. The SSL was lasing on lines  $P_{20}(8-11)$  while these RF-AR measurements were performed. Comparison of these RF-AR data with the ZP-AR data indicated that the ZP-AR profiles were suppressed, which resulted in a lower and more uniform RF-AR distribution. The gains of the low  $J$  lines  $P_1(4-6)$  and  $P_2(4-6)$  were suppressed

between 41 and 96% and the gains of the high  $J$  lines  $P_1(7-9)$  and  $P_2(7-9)$  were suppressed between 3 and 44%. The  $1 \rightarrow 0$  lines were suppressed more than the  $2 \rightarrow 1$  lines. The maximum suppression occurred between 2 and 6 mm downstream from the nozzle exit plane, near the center of the 9 mm overtone beam. There was minimal suppression of lines  $P_2(8, 9)$ . The surprising result was that the low  $J$  fundamental gains were suppressed more than the high  $J$  fundamental gains even though their upper or lower levels were not directly involved in overtone lasing. The reasons for this are discussed in Refs. 10 and 12.

Residual fundamental gain measurements at low-medium saturation with overtone mirrors of 99.7/98.0% reflectivity showed weak suppression on lines  $P_1(7)$ ,  $P_2(5)$ , and  $P_2(6)$  at axial positions between 2 and 6 mm downstream from the nozzle exit plane. There was no suppression measured for any of the other lines. These results verified the computer model's prediction of minimal fundamental gain suppression at this low level of medium saturation.<sup>10,12</sup>

Residual fundamental gain was measured at an increased level of medium saturation with overtone mirrors of 99.8/99.86% reflectivity. The intracavity flux in this case was 50% higher and  $\alpha_{\text{sat}}$  was 43.4% smaller than that of the two 99.7% reflective mirrors. The suppression obtained with the 99.8/99.86% reflective mirrors was essentially the same as that obtained with the 99.7/99.7% mirrors. This result agrees with the computer model prediction that above a reflectivity of 99.7% the RF-AR does not change significantly with increased reflectivity.<sup>10,12</sup>

Since the maximum overtone device gain length will be determined by the ability of a fully saturated overtone laser to suppress the fundamental gains and reduce amplified spontaneous emission, RFG experiments should be performed with a longer device to experimentally determine the fundamental gain suppression as a function of gain length. The high  $J$ ,  $P_2(7-9)$  lines whose upper states were directly involved in overtone lasing showed minimal suppression in the case of the 30-cm device. If this is also the case at longer gain lengths (higher medium saturation), the gains of these  $2 \rightarrow 1$  lines may present a significant scaling limitation for the overtone laser.

### Acknowledgment

This work was supported by the Strategic Defense Initiative Organization through W. J. Schafer Associates Subcontract SC-88K-33-004.

### References

- <sup>1</sup>Jeffers, W. Q., "Short Wavelength Chemical Lasers," *AIAA Journal*, Vol. 27, No. 1, 1989, pp. 64-66.
- <sup>2</sup>Smith, W., Howie, S. S., Long, J., Taylor, S., and Acebal, R., "HF Overtone Laser Device Performance Modeling and Data Correlation," Science Applications International Corp., DAAH01-86-D-0007, Marietta, GA, May 1989.
- <sup>3</sup>Duncan, W., Holloman, M., Rodgers, B., and Patterson, S., "Hydrogen Fluoride Overtone Chemical Laser Technology," AIAA Paper 89-1903, June 1989.
- <sup>4</sup>Duncan, W., Patterson, S., Graves, B., and Holloman, M., "Recent Progress in Hydrogen Fluoride Overtone Chemical Lasers," AIAA Paper 91-1480, June 1991.
- <sup>5</sup>Smith, W., and Schafer, E., "Gain Medium Considerations in the Design of Overtone Chemical Laser Resonators," AIAA Paper 91-1481, June 1991.
- <sup>6</sup>Sentman, L. H., Theodoropoulos, P. T., Nguyen, T., Carroll, D., and Waldo, R., "An Economical Supersonic cw HF Laser Testbed," AIAA Paper 89-1898, June 1989.
- <sup>7</sup>Sentman, L. H., Nguyen, T. X., Theodoropoulos, P. T., Waldo, R. E., and Carroll, D. L., "An Experimental Study of Supersonic cw HF Chemical Laser Zero Power Gain," Aeronautical and Astronautical Engineering Dept., TR 89-6 UILU Eng. 89-0506, Univ. of Illinois at Urbana-Champaign, Urbana, IL, Aug. 1989.
- <sup>8</sup>Carroll, D. L., Sentman, L. H., Theodoropoulos, P. T., Waldo, R. E., and Gordon, S. J., "Experimental Study of Continuous Wave Hydrogen-Fluoride Chemical Laser Overtone Performance," *AIAA Journal*, Vol. 31, No. 4, 1993, pp. 693-700.
- <sup>9</sup>Sentman, L. H., Theodoropoulos, P. T., Waldo, R. E., Nguyen, T., and Snipes, R., "An Experimental Study of cw HF Chemical Laser Amplifier Performance and Zero Power Gain," Aeronautical and Astronautical Engineering Dept., TR 87-6 UILU Eng 87-0506, Univ. of Illinois at Urbana-Champaign, Urbana, IL, Aug. 1987.
- <sup>10</sup>Theodoropoulos, P. T., Sentman, L. H., Carroll, D. L., Waldo, R. E., Gordon, S. J., and Otto, J. W., "Experimental and Theoretical Study of cw HF Chemical Laser Residual Fundamental Gain," Aeronautical and Astronautical Engineering Dept., TR 92-09 UILU Eng 92-0509, Univ. of Illinois at Urbana-Champaign, Urbana, IL, May 1992.
- <sup>11</sup>Smith, W., Howie, S., Long, J., Taylor, S., and Acebal, R., "Space Based Directed Energy Technology Support—Area I: Laser Device—HF Overtone Laser Performance Modeling and Data Correlation," Science Applications International Corp., DAAH01-86-D-0007, Marietta, GA, May 1989.
- <sup>12</sup>Theodoropoulos, P. T., and Sentman, L. H., "Fundamental Gain Suppression Mechanisms in a Continuous Wave Hydrogen Fluoride Overtone Laser," *AIAA Journal* (to be published).